

# Amino acid starvation promotes podocyte autophagy through mammalian target of rapamycin inhibition and transcription factor EB activation

YUANHAN CHEN<sup>1,2\*</sup>, XINGCHEN ZHAO<sup>1,2\*</sup>, JIAXIN LI<sup>3</sup>, LI ZHANG<sup>2</sup>, RUIZHAO LI<sup>2</sup>, HONG ZHANG<sup>2</sup>, RUYI LIAO<sup>2</sup>, SHUANGXIN LIU<sup>2</sup>, WEI SHI<sup>1,2</sup> and XINLING LIANG<sup>2</sup>

<sup>1</sup>The Second School of Clinical Medicine, Southern Medical University; <sup>2</sup>Division of Nephrology, Guangdong General Hospital, Guangdong Academy of Medical Sciences, Guangdong Geriatrics Institute; <sup>3</sup>Cardiac Surgical Intensive Care Unit, Guangdong Cardiovascular Institute, Guangdong General Hospital, Guangdong Academy of Medical Sciences, Guangzhou, Guangdong 510080, P.R. China

Received November 20, 2017; Accepted June 6, 2018

DOI: 10.3892/mmr.2018.9438

**Abstract.** Autophagy is important for maintaining normal physiological functions and podocyte cell homeostasis. Amino acid signaling is an important upstream signaling pathway for autophagy regulation. However, the function and the associated mechanism of amino acid signaling in podocyte autophagy is unclear. The present study used normal culture medium and amino acid deprivation medium to culture podocytes *in vitro*. Multiple methods were utilized to detect autophagic activity including western blot analysis to measure the levels of microtubule-associated protein 1 light chain 3 (LC3) II and beclin1, reverse transcription-quantitative polymerase chain reaction was performed to evaluate the levels of LC3 mRNA and transmission electron microscopy was conducted to observe autophagosomes. In addition, tandem green fluorescent protein (GFP)-monomeric red fluorescent protein (mRFP)-LC3 adenoviruses were employed to transduce podocytes to observe autophagic flux. Furthermore, the present study examined the effects of amino acid signaling on mammalian target of rapamycin (mTOR) activity and the nuclear translocation of transcription factor EB (TFEB), a core regulator of autophagy, using western blotting and immunofluorescence. The results revealed that amino acid starvation promoted the expression of LC3II and beclin1, and increased

the number of autophagosomes and autolysosomes. Amino acid starvation inhibited mTOR activity, and promoted nuclear translocation and TFEB activity. Inhibition of TFEB blocked amino acid starvation-induced autophagy. These results indicated that amino acid starvation stimulated podocyte autophagy, and thus suggested that mTOR suppression and TFEB activation may mediate amino acid starvation-induced autophagy in podocytes.

## Introduction

Autophagy is a process of degrading and recycling discarded proteins and organelles that is dependent on lysosomes. The process of autophagy involves formation of autophagosomes, fusion of autophagosomes and lysosomes into autolysosomes, and substrate degradation. This dynamic process, called autophagic flux, is crucial for maintaining intracellular homeostasis and preventing aging (1,2).

Podocytes are key components of the glomerular filtration barrier. Podocyte injury is a common pathogenesis for many glomerular diseases. Since podocytes are a type of terminally differentiated cells, their ability to regenerate after injury is weak. Therefore, self-repair mechanisms are particularly important for podocytes. Podocytes have high constitutive autophagy and podocyte-specific autophagy knockdown aggravates podocyte damage and progression of glomerular diseases (3). However, the mechanism of podocyte autophagy is not completely understood.

Amino acids (AA) are important upstream signals for autophagy regulation. Amino acid starvation (AAS) is a critical mechanism for autophagy induction, but the functions of AA in podocyte autophagy are unclear. Mammalian target of rapamycin (mTOR) is a serine/threonine phosphorylase that has key functions in intracellular regulation of cell proliferation and energy. mTOR is also important in inhibiting autophagy. Short-term AAS can block mTOR activity and relieve its inhibition of autophagy-related molecules in downstream pathways, initiating autophagy (4,5). AA signaling also regulates autophagy at the transcriptional level, such as through

---

*Correspondence to:* Professor Wei Shi or Professor Xinling Liang, Division of Nephrology, Guangdong General Hospital, Guangdong Academy of Medical Sciences, Guangdong Geriatrics Institute, 106 Zhongshan No. 2 Road, Guangzhou, Guangdong 510080, P.R. China  
E-mail: shiwei.gd@139.com  
E-mail: xinlingliang\_ggh@163.com

\*Contributed equally

**Key words:** podocytes, autophagy, amino acid, mammalian target of rapamycin, transcription factor EB

transcription factor EB (TFEB). TFEB promotes transcription of multiple genes in the autophagy process, including formation of autophagosomes, autolysosome formation and substrate degradation. As observed in HeLa cells stably expressing high levels of TFEB (6) and in HEK-293T cells (7), AAS promotes nuclear translocation of TFEB. We hypothesized that AA may also regulate podocyte autophagy via mTOR and TFEB pathways. Therefore, this study aimed to investigate the functions and mechanisms of AA signaling in podocyte autophagy.

## Materials and methods

**Cell culture and treatment.** The conditionally immortalized mouse podocyte cell line (Mouse Podocyte Clone-5, MPC-5) was a kind gift from Dr. Jochen Reiser (Rush University Medical Center, Chicago, IL, USA). Differentiated podocytes are unable to replicate, and primary podocytes would result in rapid growth arrest when culturing. The MPC-5 has overcome these difficulties, and conditionally retains a differentiation potential similar to that of podocytes *in vivo* (8), which is widely used as a cell model in research focusing on human podocyte injury. Cells were cultured as described previously (9). The recovered cells were cultured at 33°C in RPMI-1640 medium supplemented with 10% fetal bovine serum (FBS; both Gibco; Thermo Fisher Scientific, Inc., Waltham, MA, USA) and recombinant interferon (IFN)- $\gamma$  (ProSpec, Tany Technogene, Ness Ziona, Israel) for 2-3 days for proliferation. Podocytes were then transferred to 100-cm<sup>2</sup> culture dishes coated with type-I collagen (BD Bioscience, Bedford, MA, USA) in IFN- $\gamma$  free RPMI-1640 medium containing 5% FBS and cultured at 37°C for 10-13 days for differentiation. To establish an AA-starved podocyte model, differentiated podocytes were treated with AA-deprivation RPMI-1640 medium (Gibco; Thermo Fisher Scientific, Inc.) supplemented with 5% FBS for 6, 12 or 24 h. Podocytes were treated with complete RPMI-1640 medium (Gibco; Thermo Fisher Scientific, Inc.) supplemented with 5% FBS as the control group.

**Small interfering RNA (siRNA) transfection.** siRNA targeting TFEB and control siRNA were designed and synthesized by RiboBio Co. Ltd (Guangzhou, China). TFEB siRNA or control scrambled siRNA was transfected into podocytes with Lipofectamine 2000 reagent (Invitrogen, Carlsbad, CA, USA) according to the manufacturer's protocol. Podocytes were transfected for 48 h at 37°C. The sequence of siRNA used in this study was: siTFEB 5'CCATGGCCATGCTACATA TdTT-3'.

**Western blot analysis.** Podocytes were washed three times with cold phosphate-buffered saline (PBS) and lysed with lysis buffer (Beyotime Institute of Biotechnology, Shanghai, China) premixed with proteinase inhibitor (Guangzhou Genebase Bioscience, Guangzhou, China). Protein was measured using bicinchoninic acid protein quantification kits (Thermo Fisher Scientific, Inc.) and 15-30 micrograms protein was processed on 7.5-10% sodium dodecyl sulfate-polyacrylamide gels and transferred to polyvinylidene fluoride membranes (Millipore, Billerica, MA, USA). After blocking with 5% non-fat dry milk for 1 h at room temperature, membranes were incubated overnight at 4°C with primary antibodies: Rabbit anti-light chain

(LC)3A/B (1:1,000; cat. no. 4108), rabbit anti-beclin1 (1:1,000; cat. no. 3495), rabbit anti-p62 (1:1,000; cat. no. 5114), rabbit anti-phospho-p70s6k (1:1,000; cat. no. 9205; all Cell Signaling Technology, Danvers, MA, USA); rabbit anti-GAPDH (1:3,000; cat. no. AP0063; Bioworld Technology, Nanjing, China); rabbit anti-p70s6k (1:1,000; cat. no. ab32359; Abcam, Cambridge, MA, USA). Anti-rabbit IgG (1:3,000; cat. no. 31460; Thermo Fisher Scientific, Inc.) was incubated with membranes at room temperature for 1 h. Blots were treated with enhanced chemiluminescence reagent (Advansta, Menlo Park, CA, USA). Images were captured by automatic imager (General Electric, Fairfield, CT, USA). Densitometric analyses of protein bands used ImageJ software (National Institutes of Health, Bethesda, MD, USA).

**Transmission electron microscopy.** Podocytes were fixed in 2.5% glutaraldehyde. Samples were dehydrated with alcohol and post-fixed with 1% osmium tetroxide. Samples were embedded into resin (Epon 812) and cut into ultrathin slices and double stained with uranyl acetate and examined by transmission electron microscope (FEI, TECNAI 12, Lausanne, Netherlands). Numbers of autophagosomes or autolysosomes per cell were counted blind (10,11).

**Green fluorescent protein (GFP)-monomeric red fluorescent protein monomeric red fluorescent protein (mRFP)-LC3 adenovirus transduction.** Cultured podocytes were seeded onto cover slides in six-well plates. To detect autophagic flux, podocytes were transduced with tandem GFP-mRFP-LC3 adenovirus which was purchased from Hanbio Technology (Shanghai, China) as described previously (9). Podocytes were transduced with the GFP-mRFP-LC3 adenovirus at a concentration of  $1 \times 10^7$  PFU/well and incubated in RPMI-1640 medium containing 2% FBS. The transduction medium was replaced with fresh culture medium after 6 h of transduction. Treatment (with AA-deprivation RPMI-1640 medium supplemented with 5% FBS or complete RPMI-1640 medium supplemented with 5% FBS for 6 h) was performed at 24 h post-transduction.

**Immunofluorescent staining.** Cultured podocytes transduced with GFP-mRFP-LC3 adenovirus were washed with PBS and fixed with 4% paraformaldehyde and permeabilized using 0.1% Triton X-100 for 10 min. After washing with PBS, podocytes were stained with DAPI (Sigma, St. Louis, MO, USA) for 10 min at room temperature. Photomicrographs were taken by confocal laser scanning microscopy (KS 400; Zeiss, Postfach, Germany). GFP signal is sensitive to acidic proteolytic conditions of the lysosome lumen, whereas mRFP is more stable (12). Colocalization of GFP and mRFP indicates autophagosomes (yellow). MRFP signal alone indicates autolysosomes (red).

To observe subcellular localization of TFEB, 4% paraformaldehyde was used to fix cells at room temperature for 15 min. Samples were permeabilized using 0.1% Triton X-100 for 10 min and blocked with 5% bovine serum albumin at room temperature for 30 min followed by incubating overnight at 4°C with rabbit anti-TFEB antibody (1:200; cat. no. A303-673A; Bethyl, Montgomery, TX, USA.). Samples were washed 3 times with PBS and incubated with goat

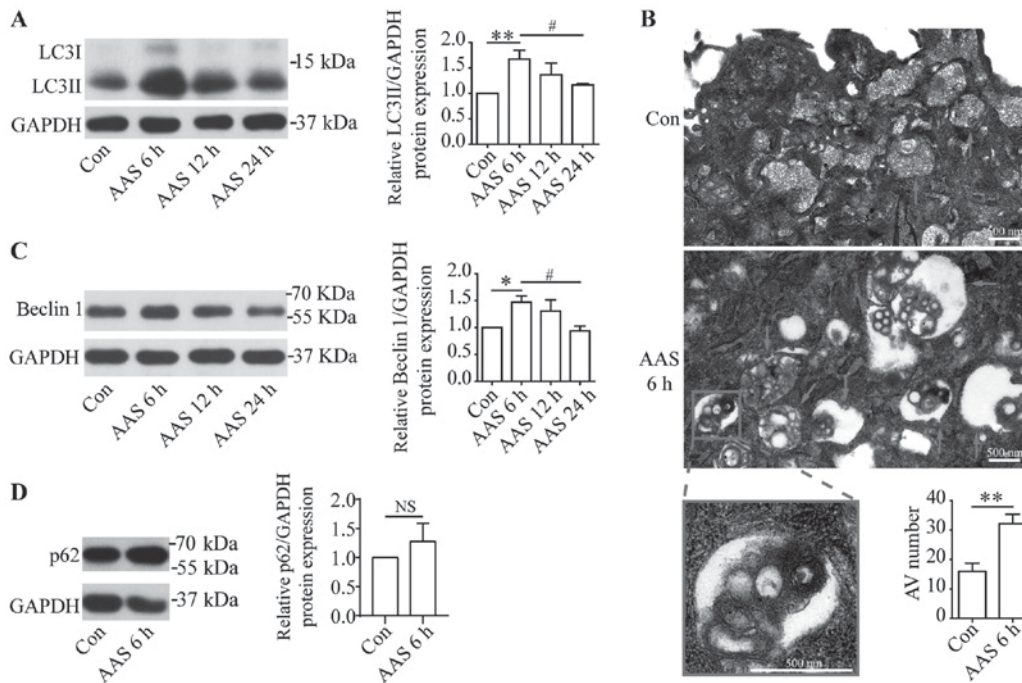


Figure 1. Amino acid starvation stimulates autophagy in podocytes. (A) Western blots of LC3II in cultured podocytes: Untreated (Control) or amino acid starved for the indicated times. AAS induced LC3II expression in a time-dependent manner. (B) Transmission electron microscopy of the cultured podocytes treated, as indicated. AAS for 6 h increased the number of autophagic vacuoles (indicated by arrows) in podocytes. Scale bars, 500 nm. (C) Western blot of beclin1 in cultured podocytes: Untreated (Control) or amino acid starved for the indicated times. AAS induced beclin1 expression in a time-dependent manner. (D) Western blot of p62 in cultured podocytes: Untreated (Control) or amino acid starved for 6 h. Values are presented as the mean  $\pm$  standard error of the mean (n=3). \*\*P<0.01 vs. control; #P<0.05 vs. AAS 6 h. NS, non-significant; LC3, microtubule-associated protein 1 light chain 3; Con, control; AAS, amino acid starvation; AV, autophagic vacuoles.

anti-rabbit AlexaFluor 555 antibody (1:200; cat. no. A32732; Thermo Fisher Scientific, Inc.) for 1 h at room temperature. After washing with PBS, podocytes were stained with DAPI for 10 min at room temperature and analyzed by confocal laser scanning microscopy.

**Reverse transcription-quantitative polymerase chain reaction (RT-qPCR).** Total RNA samples were extracted using a TRIzol RNA isolation system (Invitrogen). Purity and concentration of mRNA samples were measured using a NanoDrop 2000 spectrophotometer (Thermo Fisher Scientific, Inc., Wilmington, DE, USA). Samples were reverse transcribed (RT) into cDNAs using PrimeScript™ RT reagent kits (Takara Biotechnology, Shiga, Japan). cDNAs were used for RT-qPCR analysis using a Power SYBR Green PCR Master Mix (Takara Biotechnology). qPCR was performed with 2  $\mu$ l aliquots of cDNA (10 ng/ $\mu$ l) using specific primer pairs. Primers were as follows: LC3A forward, 5'-GACCGCTGTAAGGAGGTGC-3' and reverse, 5'-CTTGACCACTCGCTCATGTTA-3'; LC3B forward, 5'-TTATAGACGATACAAGGGGAG-3' and reverse, 5'-CGCCGTCTGATTATCTTGATGAG-3'; GAPDH forward, 5'-AGGTCGGTGTGA ACG GAT TTTG-3' and reverse, 5'-TGTAGACCATGTAGTTGAGGTCA-3'. Samples were amplified by 95°C for 2 min, 40 cycles of 95°C for 30 sec, 95°C for 5 sec, 60°C for 5 sec, and a 72°C for 10 min. Data were calculated using the  $2^{-\Delta\Delta C_t}$  method (13).

**Statistical analysis.** Values are expressed as mean  $\pm$  standard error of the mean. Data were analyzed by the statistical package SPSS for Windows version 21.0 (IBM Corp., Armonk,

NY, USA). Multiple comparisons were performed with one-way analysis of variance followed by the least-significant difference post hoc test. Data from two groups were compared by Student's t-test. P<0.05 was considered to indicate a statistically significant difference. All experimental procedures were repeated at least three times.

## Results

**AAS promotes podocyte autophagy.** To determine if AAS regulated podocyte autophagy, we used AA deprivation medium and normal medium to culture podocytes for indicated times. Western blots showed that after 6-h AAS, LC3II, an autophagosome marker, increased in podocytes significantly to peak level (Fig. 1A). After 12-h AAS treatment, LC3II levels were still higher than the control group, but decreased compared with 6-h AAS treatment (Fig. 1A). After 24-h AAS, LC3II levels returned to baseline (Fig. 1A). The effect of AA signal on autophagy was further studied by transmission electron microscopy, which showed that 6-h AAS promoted formation of autophagic vacuoles in podocytes (Fig. 1B). Western blots found that the changes for beclin1, a marker of autophagy initiation, at different AAS times coincided with LC3II (Fig. 1C). These results suggested that AAS increased autophagic activity. p62 serves as a substrate of autophagy. In certain settings, stimulation of autophagy correlates with decreased level of p62 (14). We investigated the p62 expression by western blots and the results showed that p62 did not altered significantly under the stimulation of AAS for 6 h (Fig. 1D). This is inconsistent with the increased autophagic activity

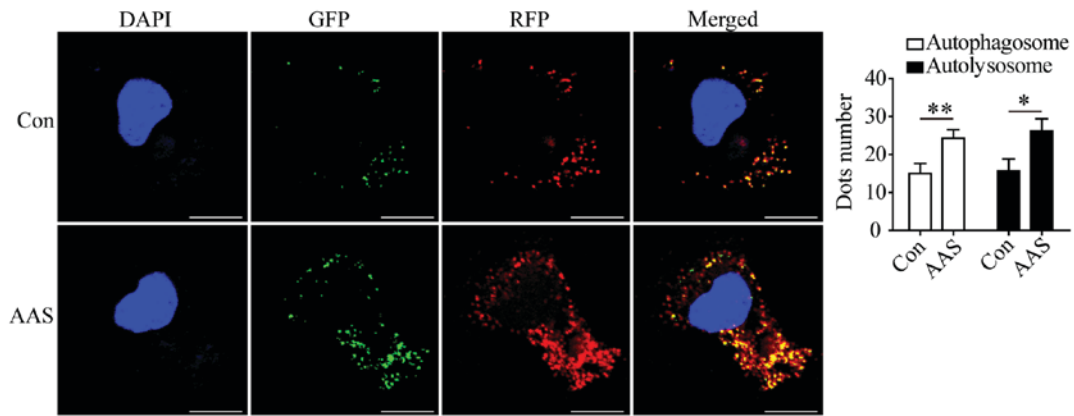


Figure 2. Amino acid starvation induces autophagic flux in podocytes. Confocal laser scanning microscopy images of cultured podocytes: Untreated (Control) or amino acid starved for 6 h, transduced with GFP-mRFP-LC3 adenovirus. AAS increased autophagosomes (green staining) and autolysosomes (red staining). Scale bars, 20  $\mu$ m. Values are presented as the mean  $\pm$  standard error of the mean (n=20). \*P<0.05 and \*\*P<0.01 vs. control. GFP-mRFP-LC3, tandem green fluorescent protein-monomeric red fluorescent protein-microtubule associated protein 1 light chain 3; Con, control; AAS, amino acid starvation; DAPI, 4',6-diamidino-2-phenylindole.

under AAS stimulation (Fig. 1A-C), indicating that in addition to autophagy, there are other factors that can affect the level of p62 in this AAS-stimulated model.

**AAS promotes autophagic flux.** We evaluated the effect of AAS on autophagic flux in podocytes. The AAS-induced enhancement of beclin1 expression (Fig. 1C) suggested the AAS-induced increase of autophagosomes (Fig. 1A and B) was related to the enhancement of autophagy initiation. Moreover, in podocytes transduced with GFP-mRFP-LC3 adenovirus, AAS increased the number of autophagosomes (Fig. 2) and autolysosomes (Fig. 2). These results indicated that AAS contributed to formation and turnover of autophagosomes.

**mTOR was inactivated under AAS.** We investigated the molecular mechanisms underlying AAS regulation of autophagy in podocytes. mTOR is a well-known negative regulator of autophagy. p70S6k (p70 ribosomal protein S6 kinase) is the phosphorylation substrate of mTOR, and the level of phosphorylated p70S6k reflects mTOR activity (15). Western blots showed that 6-h AAS inhibited mTOR activity (Fig. 3). The mTOR activity gradually recovered after 12-h AAS (Fig. 3), contrary to the changes of autophagy after AAS. This result suggested that AAS promoted autophagy by inhibiting mTOR activity.

**TFEB-mediated AAS-induced autophagy.** The above-mentioned results demonstrated AAS promote autophagic flux at multiple steps. We have reported previously that TFEB promoted podocyte autophagy through enhancing autophagosome formation and degradation (16). Thus, we studied the role of TFEB in AAS-induced autophagy in cultured podocytes. AAS promoted nuclear translocation of TFEB (Fig. 4A) and raised levels of mRNA (Fig. 4B) and protein (Fig. 1A) for LC3B, a target gene of TFEB (6,16), indicating increased TFEB activity by AAS. Next, we utilized TFEB siRNA to observe whether TFEB mediated AAS-induced autophagy. As we reported previously, TFEB siRNA significantly inhibited the expression of TFEB at mRNA, total protein and nuclear protein level in cultured podocytes (16). The present study found that TFEB siRNA

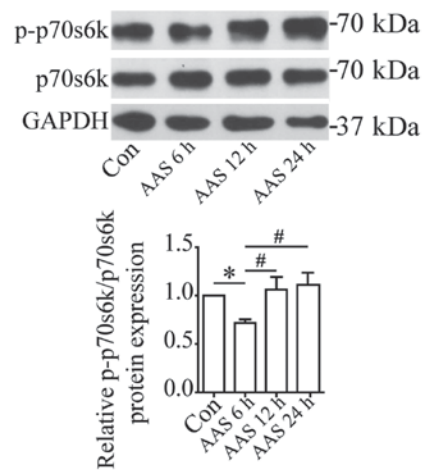


Figure 3. Amino acid starvation inhibits mTOR activity in podocytes. Western blotting of p-p70s6k and p70s6k in cultured podocytes: Untreated (Control) or amino acid starved for the indicated times. AAS 6 h decreased the ratio of p-p70s6k to p70s6k. Values are presented as the mean  $\pm$  standard error of the mean (n=4). \*P<0.05 vs. control; #P<0.05 vs. AAS 6 h. mTOR, mammalian target of rapamycin; p70s6k, p70 ribosomal protein S6 kinase; p-, phosphorylated; Con, control; AAS, amino acid starvation.

blocked AAS-induced LC3II upregulation (Fig. 4C and D), indicating TFEB mediated the AAS-induced autophagy in podocytes.

Moreover, p62 serves as a target gene of TFEB (6,16). We found that TFEB siRNA decreased the p62 protein expression in cultured podocytes (Fig. 4E). As AAS increased the nuclear transportation and activity of TFEB, these results suggested a potential role of TFEB in regulating p62 levels in AAS-stimulated podocytes.

## Discussion

The present study investigated the effect of AA on podocyte autophagy. We found that AAS promoted autophagy in podocytes. AAS affected autophagy through at least two pathways, inhibiting mTOR activity and promoting TFEB nuclear translocation and activity.

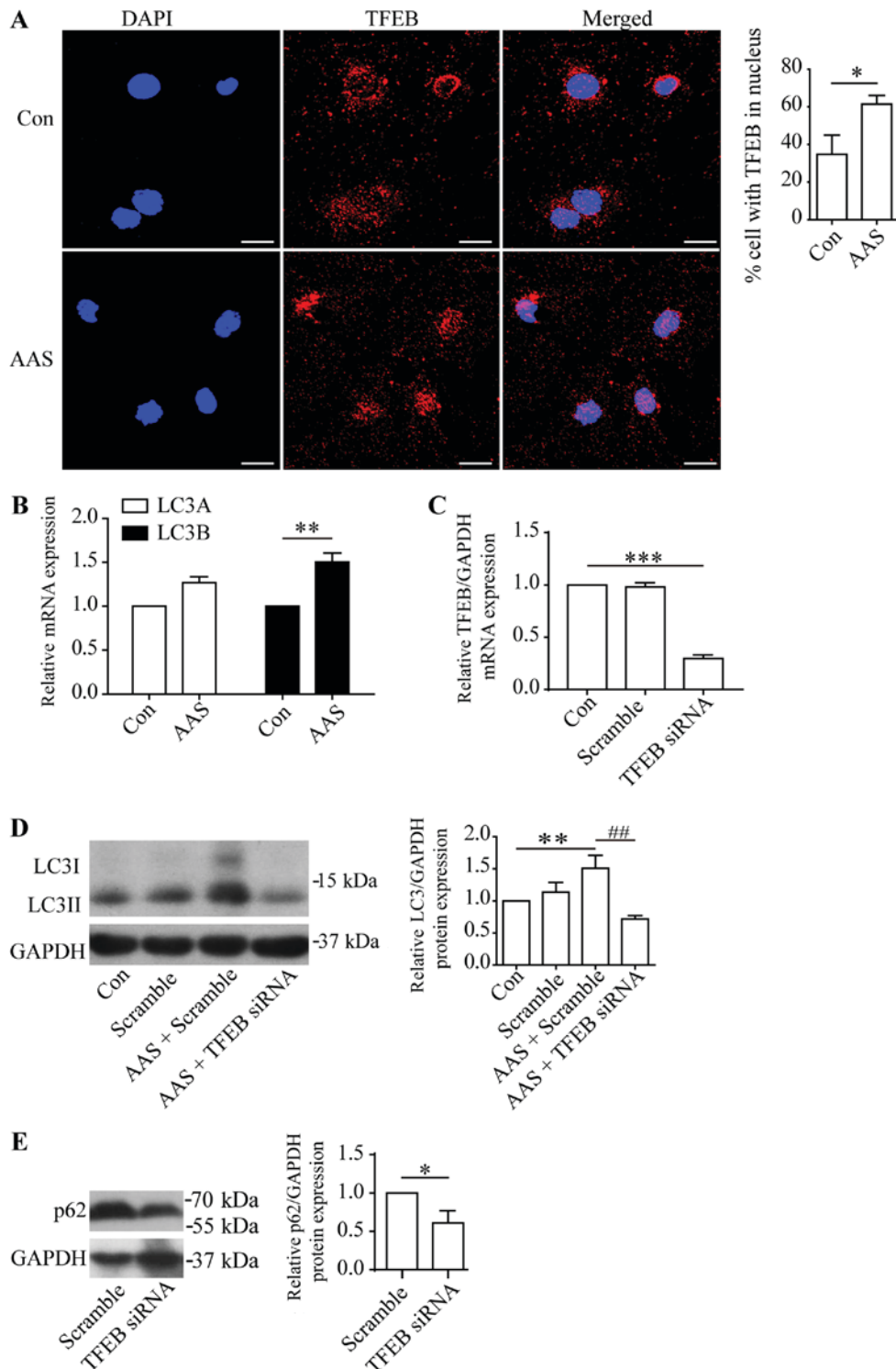


Figure 4. TFEB-mediated amino acid starvation induces autophagy in podocytes. (A) Immunofluorescence staining for TFEB (red staining) and DAPI (blue staining) in cultured podocytes: Untreated (Control) or amino acid starved for 6 h. AAS enhanced TFEB nuclear translocation. Scale bars, 20  $\mu$ m. (B) RT-qPCR analyses of LC3A and LC3B in cultured podocytes: Untreated (Control) or amino acid starved for 6 h. (C) RT-qPCR of TFEB mRNA expression. (D) Western blotting of LC3II in podocytes transfected with scrambled or TFEB siRNA: Untreated (Control) or amino acid starved for 6 h. TFEB siRNA blocked AAS-induced autophagy. \* $P < 0.05$  and \*\* $P < 0.01$  vs. control; ### $P < 0.01$  vs. AAS + scrambled. (E) Western blotting of p62 in podocytes transfected with scrambled or TFEB siRNA. TFEB siRNA decreased the p62 expression. Values are presented as the mean  $\pm$  standard error of the mean (n=3). \* $P < 0.05$  vs. Scramble. TFEB, transcription factor EB; DAPI, 4',6-diamidino-2-phenylindole; Con, control; AAS, amino acid starvation; LC3, microtubule-associated protein 1 light chain 3; siRNA, small interfering RNA; RT-qPCR, reverse transcription-quantitative polymerase chain reaction; Scramble, scrambled siRNA.

AA regulation of autophagy was time-dependent: 6 h of AAS promoted podocyte autophagy to reach peak level. With AAS over 6 h, autophagy decreased gradually and resumed basic levels at 24 h. The changes of mTOR activity were

time-dependent under AAS, but opposite of autophagy. The changes of mTOR under AAS were similar to a study that found that short-term nutrient deprivation inhibits the mTOR signaling pathway in normal rat kidney cells, but mTOR was

reactivated with prolonged starvation (17). This result may be due to starvation-induced autophagy leading to decomposing and recycling autophagy substrates, which reactivates mTOR (17).

In addition to post-transcriptional regulation of autophagy through mTOR, AA signaling also regulates autophagy transcriptionally. Our study found that AAS promoted nuclear translocation of TFEB and increased TFEB activity in podocytes. Moreover, TFEB siRNA inhibited the increased autophagy induced by AAS in podocytes. These results demonstrated that AAS also contributed to podocyte autophagy via activating TFEB.

Autophagy is a dynamic and multi-step process orchestrated by series of proteins. Thus, multi-dimensional assessments of autophagy are recommended to interpret it. The present study utilized western blots to detect LC3 and beclin1, GFP-mRFP-LC3 fluorescent probe and TEM to examine autophagy, which all suggested an increasing autophagic activity by AAS. Autophagy upregulation often correlates with enhanced autolysosome-mediated degradation of substrates such as p62 (14). We also investigated the level of p62 under AAS stimulation. However, p62 did not altered significantly under AAS stimulation for 6 h, which is inconsistent with the AAS-induced upregulation of autophagic activity. Moreover, p62 serves as a target gene of TFEB (6) and we validated the role of TFEB in regulating p62 protein levels in podocytes. We also observed that AAS increased TFEB activity. These results suggested that in this AAS-stimulated model, p62 level was affected not only by the increased activity of autophagy (led to p62 downregulation) but also by increased activation of TFEB (led to p62 upregulation). Therefore, p62 may not serve as an effective marker for autophagy degradation in this model.

Autophagy in podocytes has been studied often, but the level of autophagy in podocytes is too weak to be measured precisely by commonly used detection methods. Nutritional starvation is a common method to increase autophagic activity (11). Previous studies reported serum starvation (18), Hanks solution induced starvation (11) or EBSS solution induced starvation (19) promoted podocyte autophagy. These were autophagy induction models induced by a variety of nutrient deficiencies. Our study showed that, among these nutrient components, AA were a key component in inducing autophagy. In addition, AAS induced high autophagic activity in cultured podocyte model, providing a new tool for studying podocyte autophagy.

Studies found that podocyte autophagy damage occurs in many glomerular diseases, contributing to pathogenesis and progression of renal disease such as diabetic nephropathy (20), focal segmental glomerulosclerosis (11) and membranous nephropathy (21). Restoring podocyte autophagy levels is an urgent problem to be solved. Previous studies found that serum concentrations of various AAs in patients with chronic kidney disease and diabetic nephropathy are abnormal (22,23). Very-low-protein diets (AA restriction) alleviated renal injury and restored autophagy levels in diabetic rats (24). Our results suggested that manipulation of local AA concentrations in podocytes may be a potential method for regulating podocyte autophagy.

In conclusion, this study found that short-term AAS promoted podocyte autophagy by inhibiting mTOR and promoting TFEB activity.

## Acknowledgements

The authors would like to thank Professor Jochen Reiser (Rush University Medical Center) for providing the podocyte cell line.

## Funding

The present study was supported by the National Natural Science Foundation of China (grant nos. 81770733 and 81270784).

## Availability of data and materials

The datasets used and analyzed during the current study are available from the corresponding author on reasonable request.

## Authors' contributions

XL and WS conceived the present study. YC, XZ and WS analyzed the data. YC, XZ and XL wrote the manuscript. YC, XZ, JL, LZ, RL, HZ, RL, SL, WS and XL were all involved in performing the experiments and had final approval of the version to be published.

## Ethics approval and consent to participate

Not applicable.

## Patient consent for publication

Not applicable.

## Competing interests

The authors declare that they have no competing interests.

## References

- Mizushima N and Komatsu M: Autophagy: Renovation of cells and tissues. *Cell* 147: 728-741, 2011.
- Mizushima N, Levine B, Cuervo AM and Klionsky DJ: Autophagy fights disease through cellular self-digestion. *Nature* 451: 1069-1075, 2008.
- Hartleben B, Gödel M, Meyer-Schwesinger C, Liu S, Ulrich T, Köbler S, Wiech T, Grahhammer F, Arnold SJ, Lindenmeyer MT, *et al*: Autophagy influences glomerular disease susceptibility and maintains podocyte homeostasis in aging mice. *J Clin Invest* 120: 1084-1096, 2010.
- Sancak Y, Peterson TR, Shaul YD, Lindquist RA, Thoreen CC, Bar-Peled L and Sabatini DM: The Rag GTPases bind raptor and mediate amino acid signaling to mTORC1. *Science* 320: 1496-1501, 2008.
- Jin G, Lee SW, Zhang X, Cai Z, Gao Y, Chou PC, Rezaeian AH, Han F, Wang CY, Yao JC, *et al*: Skp2-mediated RagA ubiquitination elicits a negative feedback to prevent amino-acid-dependent mTORC1 hyperactivation by recruiting GATOR1. *Mol Cell* 58: 989-1000, 2015.
- Settembre C, Di Malta C, Polito VA, Garcia Arencibia M, Vetrini F, Erdin S, Erdin SU, Huynh T, Medina D, Colella P, *et al*: TFEB links autophagy to lysosomal biogenesis. *Science* 332: 1429-1433, 2011.
- Settembre C, Zoncu R, Medina DL, Vetrini F, Erdin S, Erdin S, Huynh T, Ferron M, Karsenty G, Vellard MC, *et al*: A lysosome-to-nucleus signalling mechanism senses and regulates the lysosome via mTOR and TFEB. *EMBO J* 31: 1095-1108, 2012.

8. Mundel P, Reiser J, Zúñiga Mejía Borja A, Pavenstädt H, Davidson GR, Kriz W and Zeller R: Rearrangements of the cytoskeleton and cell contacts induce process formation during differentiation of conditionally immortalized mouse podocyte cell lines. *Exp Cell Res* 236: 248-258, 1997.
9. Tan X, Chen Y, Liang X, Yu C, Lai Y, Zhang L, Zhao X, Zhang H, Lin T, Li R and Shi W: Lipopolysaccharide-induced podocyte injury is mediated by suppression of autophagy. *Mol Med Rep* 14: 811-818, 2016.
10. Wei Q and Dong Z: HDAC4 blocks autophagy to trigger podocyte injury: Non-epigenetic action in diabetic nephropathy. *Kidney Int* 86: 666-668, 2014.
11. Zeng C, Fan Y, Wu J, Shi S, Chen Z, Zhong Y, Zhang C, Zen K and Liu Z: Podocyte autophagic activity plays a protective role in renal injury and delays the progression of podocytopathies. *J Pathol* 234: 203-213, 2014.
12. Inoki K, Mori H, Wang J, Suzuki T, Hong S, Yoshida S, Blattner SM, Ikenoue T, Rüegg MA, Hall MN, *et al*: mTORC1 activation in podocytes is a critical step in the development of diabetic nephropathy in mice. *J Clin Invest* 121: 2181-2196, 2011.
13. Livak KJ and Schmittgen TD: Analysis of relative gene expression data using real-time quantitative PCR and the 2(-Delta Delta C(T)) method. *Methods* 25: 402-408, 2001.
14. Klionsky DJ, Abdelmohsen K, Abe A, Abedin MJ, Abeliovich H, Acevedo Arozena A, Adachi H, Adams CM, Adams PD, Adeli K, *et al*: Guidelines for the use and interpretation of assays for monitoring autophagy (3rd edition). *Autophagy* 12: 1-222, 2016.
15. Holz MK, Ballif BA, Gygi SP and Blenis J: mTOR and S6K1 mediate assembly of the translation preinitiation complex through dynamic protein interchange and ordered phosphorylation events. *Cell* 123: 569-580, 2005.
16. Zhao X, Chen Y, Tan X, Zhang L, Zhang H, Li Z, Liu S, Li R, Lin T, Liao R, *et al*: Advanced glycation end-products suppress autophagic flux in podocytes by activating mammalian target of rapamycin and inhibiting nuclear translocation of transcription factor EB. *J Pathol* 245: 235-248, 2018.
17. Yu L, McPhee CK, Zheng L, Mardones GA, Rong Y, Peng J, Mi N, Zhao Y, Liu Z, Wan F, *et al*: Termination of autophagy and reformation of lysosomes regulated by mTOR. *Nature* 465: 942-946, 2010.
18. Fang L, Li X, Luo Y, He W, Dai C and Yang J: Autophagy inhibition induces podocyte apoptosis by activating the pro-apoptotic pathway of endoplasmic reticulum stress. *Exp Cell Res* 322: 290-301, 2014.
19. Mao N, Tan RZ, Wang SQ, Wei C, Shi XL, Fan JM and Wang L: Ginsenoside Rg1 inhibits angiotensin II-induced podocyte autophagy via AMPK/mTOR/PI3K pathway. *Cell Biol Int* 40: 917-925, 2016.
20. Tagawa A, Yasuda M, Kume S, Yamahara K, Nakazawa J, Chin-Kanasaki M, Araki H, Araki S, Koya D, Asanuma K, *et al*: Impaired podocyte autophagy exacerbates proteinuria in diabetic nephropathy. *Diabetes* 65: 755-767, 2016.
21. Liu WJ, Li ZH, Chen XC, Zhao XL, Zhong Z, Yang C, Wu HL, An N, Li WY and Liu HF: Blockage of the lysosome-dependent autophagic pathway contributes to complement membrane attack complex-induced podocyte injury in idiopathic membranous nephropathy. *Sci Rep* 7: 8643, 2017.
22. Laidlaw SA, Berg RL, Kopple JD, Naito H, Walker WG and Walser M: Patterns of fasting plasma amino acid levels in chronic renal insufficiency: Results from the feasibility phase of the Modification of Diet in Renal Disease Study. *Am J Kidney Dis* 23: 504-513, 1994.
23. Pena MJ, Lambers Heerspink HJ, Hellemons ME, Friedrich T, Dallmann G, Lajer M, Bakker SJ, Gansevoort RT, Rossing P, de Zeeuw D and Roscioni SS: Urine and plasma metabolites predict the development of diabetic nephropathy in individuals with Type 2 diabetes mellitus. *Diabet Med* 31: 1138-1147, 2014.
24. Kitada M, Ogura Y, Suzuki T, Sen S, Lee SM, Kanasaki K, Kume S and Koya D: A very-low-protein diet ameliorates advanced diabetic nephropathy through autophagy induction by suppression of the mTORC1 pathway in Wistar fatty rats, an animal model of type 2 diabetes and obesity. *Diabetologia* 59: 1307-1317, 2016.



This work is licensed under a Creative Commons Attribution-NonCommercial-NoDerivatives 4.0 International (CC BY-NC-ND 4.0) License.